

# INTEGRATED ANALYSIS BY GEOPHYSICAL AND SPATIAL DATA TO IDENTIFY THE FORMATION OF KEPUHLEGUNDI HOT SPRING ON BAWEAN ISLAND

M. E. D. Rafi<sup>1</sup>, M. H. M Fajar<sup>1,\*</sup>, F. Ulumuddin<sup>1</sup>, and M. S. Purwanto<sup>1</sup>

<sup>1</sup>Department of Geophysical Engineering, Institut Teknologi Sepuluh Nopember, Surabaya, Indonesia

\* **Correspondence to:** M. Haris Miftakhul Fajar, mharismf@geofisika.its.ac.id.

**Abstract:** Bawean Island is a result of volcanic activity in the back-arc volcanism zone located on the north side of Java Island. Bawean Island was formed due to the geological structure being controlled by the Paleogene-Neogene tectonic line in the Meratus Pattern. The mantle tearing resulted in the formation of the Bawean Arc. The Kepuhlegundi Hot Spring is a component of the volcanism product on Bawean Island. To analyze the formation of hot springs in more detail, we conducted magnetic method measurements and integrated the data with gravity satellite and Fault Fracture Density (FFD) methods. The three methods were used to determine the continuity of the mapped geological structures surrounding the hot springs. The FFD method can be used to map the weak zone of the hot spring, which is caused by the lineament surrounding it. The magnetic and gravity methods reveal anomalous contrasts that extend towards the hot springs in the direction of the structure. The magnetic and gravity methods reveal anomalous contrasts that extend towards the hot springs in the direction of the structure. Based on regional anomaly analysis, spectrum analysis indicates that the structure is located at a shallow depth of 15 to 80 meters. The drawing in each method shows a dominant orientation in the Northeast-Southwest direction, which corresponds to the orientation of the Meratus Structure Pattern. Kepuhlegundi Hot Spring is formed due to the control of geological structures, allowing hot fluids to flow through fractures as an aquifer.

**Keywords:** bawean, hot spring, geological structure, fault fracture density, magnetic, gravity, aquifer.

**Citation:** Rafi, M. E. D., M. H. M Fajar, F. Ulumuddin, and M. S. Purwanto (2024), Integrated Analysis by Geophysical and Spatial Data to Identify the Formation of Kepuhlegundi Hot Spring on Bawean Island, *Russian Journal of Earth Sciences*, 24, ES3007, EDN: JIQGXN, <https://doi.org/10.2205/2024es000913>

## RESEARCH ARTICLE

Received: 18 March 2024

Accepted: 21 May 2024

Published: 15 August 2024



**Copyright:** © 2024. The Authors. This article is an open access article distributed under the terms and conditions of the Creative Commons Attribution (CC BY) license (<https://creativecommons.org/licenses/by/4.0/>).

## 1. Introduction

Bawean Island is located on the north of Java Island, Indonesia, which was formed due to volcanic activity. The island is in a region of Quaternary back-arc volcanism [Usman *et al.*, 2010]. Tectonic processes initiated volcanic activity in this area during the Pre-Paleogene period, forming graben structures in the basement. Magma rises to the surface through fractures in the structures formed [Hendratno and Khoir, 2019]. The volcanic rocks of Bawean Island have characteristics indicating that they originate from two distinct magmas: one resulting from the subduction of the Indo-Australian Ocean Plate at the Eurasian Plate boundary, and the other from magma in the mantle. This suggests that Bawean Island is a Back Arc Volcanism zone with a subduction depth of up to 600 km [Setijadji *et al.*, 2006].

Kepuhlegundi Hot Spring is one of the many hot springs scattered across some islands as a manifestation of volcanic activity. When a heat source such as intrusion or magma heats an aquifer in the subsurface, hot springs can form [Rosli *et al.*, 2022]. Geological structures, such as faults or fractures, can control the occurrence of hot springs by causing hot fluids to flow in weak zones until they reach the surface [Bense *et al.*, 2013]. Through the geological conditions of the hot springs, research was conducted on subsurface conditions to understand comprehensively and deeply the control of geological structures in their formation, which has not been studied before. This research is expected to be

the preliminary stage in the process of potential geothermal development, especially the potential that can be explored and validated by the geological conditions that have been mapped previously based on geophysical and spatial analysis.

Spatial data analysis can be used to mapping the weak zone through Fault Fracture Density (FFD), which is typically formed by structural presence, it is important to note that FFD is a form of remote sensing [Danakusumah and Suryantini, 2020]. Geophysical measurements were conducted through ground magnetic surveys in the vicinity of the hot spring area, oriented towards the regional structure of Bawean Island. The magnetic method is expected to effectively reveal subsurface conditions, particularly the geological structures that control geothermal systems. Volcanic rocks predominantly make up the research area and are expected to show a strong magnetic response [Alvarez and Yutis, 2015]. The magnetic method and the gravity method were also combined to make it easier to figure out what structures are below the ground, get more accurate results, and get a better picture of how hot springs work. This is because both methods are effective in determining the geometry of subsurface structures [Araffa et al., 2018; Sismanto et al., 2018]. Using the methods can be a preliminary stage in understanding the potential of geothermal, especially in utilizing open source data and field data that is regional in nature, so that it can be a reference in detailing the next research.

## 2. Geological Setting

The Bawean island is located on the Muria-Bawean volcanic back-arc line, which is a type of back-arc volcanism. The Bawean Arc is a plateau formed by the Muria-Bawean Back Arc Volcanic Line, which bisects the North Basin of East Java [van Bemmelen, 1949]. The Bawean Arc Volcanic Line follows the same direction as the Paleogene-Neogene tectonic line in the Meratus Pattern, which extends from the north of Mount Muria to the Meratus Mountains in South Kalimantan. Both lines run in a northeast-southwest (NE-SW) direction [Hamilton, 1974; Pulonggono and Martodjojo, 1994]. Tectonic processes trigger the tearing of the mantle layer during the formation of graben structures in pre-Paleogene bedrock. This process causes magma to rise to the surface and form the Bawean Arc [Hendratno and Khoir, 2019]. The formation of graben is initiated by the Paleogene Extensional Rifting period, a tectonic event that results in basin formation with hydrocarbon potential. This is followed by the Neogene Compression Wrenching period, which is characterized by pressure that causes magma to rise and form Bawean Island. [Hutubessy, 2003; Sidarto and Sanyoto, 1999]. Geothermal systems can form in the back-arc basin area due to rollback and pull-apart subduction mechanisms, which trigger the formation of geological structures in the subsurface. This creates a fracture system that serves as a pathway for hot fluids [Siringoringo et al., 2024]. The formation of hot springs in non-volcanic areas, such as Kepuhlegundi Hot Spring, can occur due to the release of water and fluids from slab sediments and rocks to the mantle boundary because of magmatic fluids originating in the subducting ocean plate [Hosono and Yamanaka, 2021].

Based on the structural pattern of the Java Sea (Figure 1), Bawean Island follows the Meratus Pattern, with a structural orientation that tends towards the northeast-southwest direction. Tectonic processes have shaped the complex structure that formed Mount Bawean [Puswanto et al., 2022]. These processes include extensional rifting during the Paleogene period, compressional wrenching during the Neogene period, and compressional thrust-folding during the Plio-Pleistocene period [Suprijadi, 1992; Usman, 2012]. The geological structure on Bawean Island tends to be a sinistral fault with a northeast – southwest orientation, following the Meratus Pattern structure [Arifin and Lugra, 2016].

Regional structure controls the formation of Bawean Island, resulting in a local surface structure with a consistent direction. Geological structure plays a significant role in the formation of hot springs. Geological structures, such as faults, can cause secondary structures to form around the fault line [Choi et al., 2016]. Secondary structures, such as fractures, can form a damage zone that increases the rock's permeability. This allows hot fluids to flow through the gaps in the fracture zone [Keegan-Treloar et al., 2022].

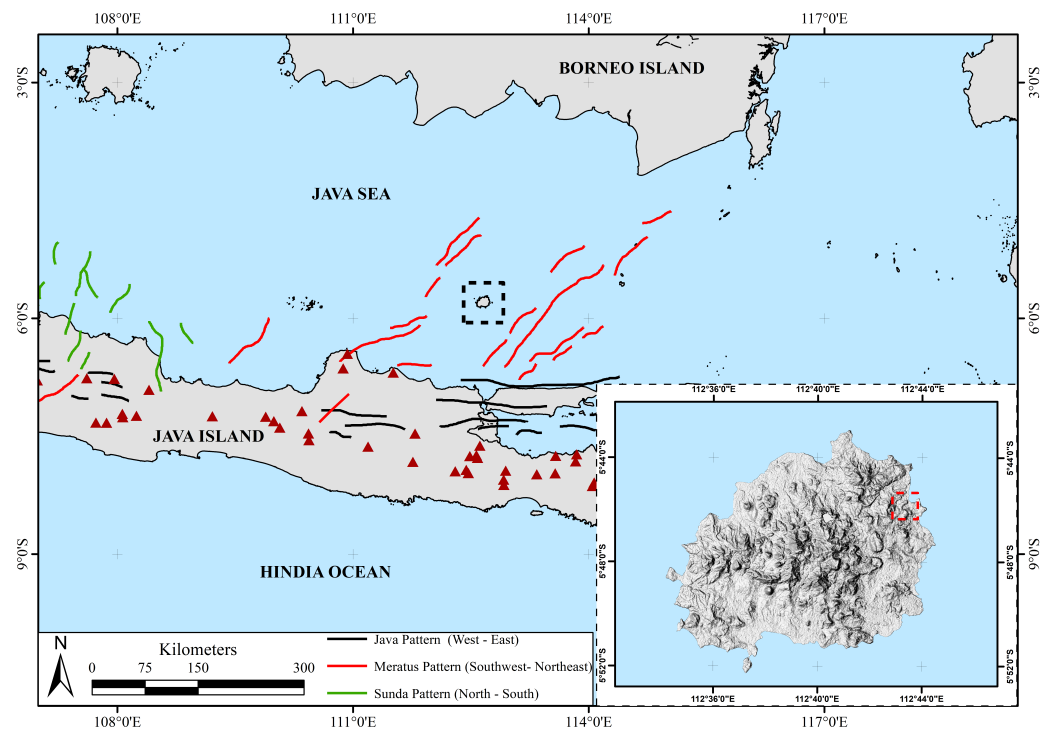


**Figure 1.** The map displays the structure pattern of Java Island with the Meratus Pattern (red line) passing through Bawean Island (dashed line), modified from [Pulonggono and Martodjojo, 1994].

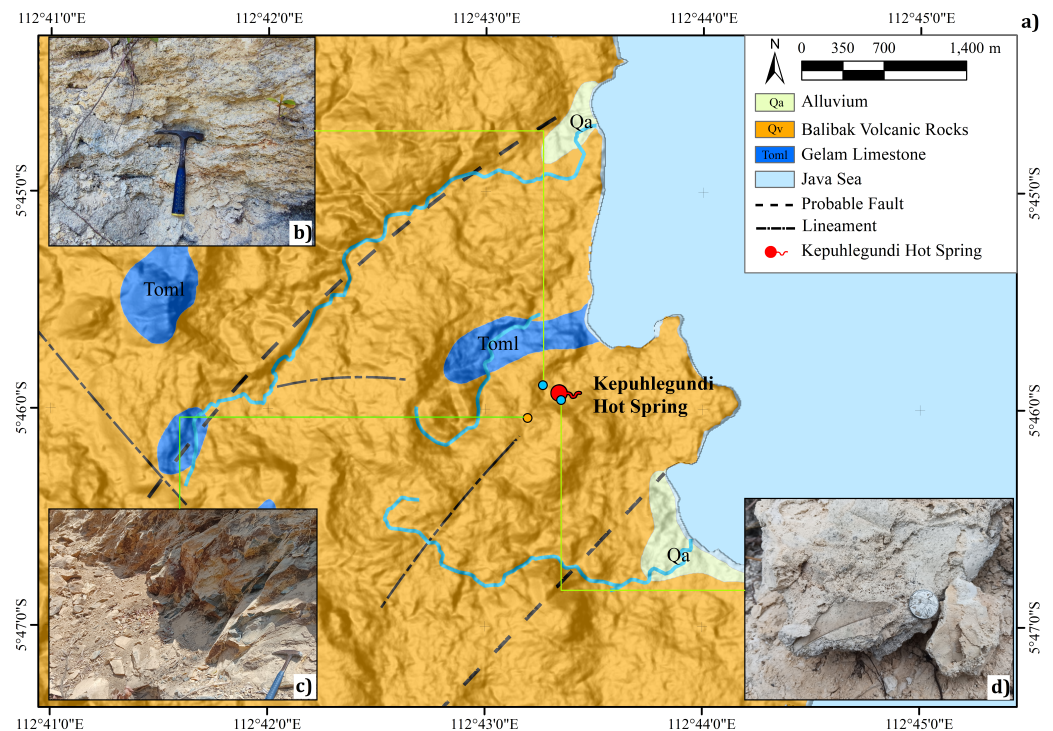


**Figure 2.** a) Geological map showing lithologies, lineament, and faults in the area, modified from [Aziz et al., 1993] b) Outcrops of travertine deposits from hot springs c) Volcanic rock outcrops in the form of lava with the type of andesite – basaltic d) Fossilized leaf molds in travertine deposits around hot springs.

The geological map of the Bawean sheet (scale 1 : 100,000) shows that marine sedimentary rocks, volcanic rocks, and alluvial deposits make up the research area (Figure 2a).

These rocks are estimated to be from the Holocene to late Oligocene periods [Aziz *et al.*, 1993]. The Gelam Limestone Formation (Toml) consists of reef limestone, clastic limestone, and crystalline limestone. These rocks are marine sedimentary products that formed during the late Oligocene age. The Balibak Volcanic Rocks (Qv) consist of alternating layers of lava, volcanic breccia, and tuff, overlying the Quaternary age (Figure 2b). The volcanic rocks on Bawean Island have a more basaltic nature compared to the volcanic rocks found in Quaternary volcanoes on Java Island. This is caused by the process of mixing two different magmas (self-mixing) between the Indian-Australian subduction plate and the magma. [Hafizh, 2022]. Travertine deposits (Figure 2c) form around the hot springs as carbonate hydrothermal sediments precipitate from solutions in the soil and water table [Luo *et al.*, 2021; Shiraishi *et al.*, 2020]. The results of travertine deposits from hot springs have a wide distribution and the field also found the presence of fossil leaf molds in these deposits (Figure 2d), which can indicate that they have a young rock age period. In groundwater systems in volcanic areas, lapilli tuff rocks have a high hydraulic conductivity value and can become aquifers or permeable layers, whereas lava rocks become impermeable layers [Fajar *et al.*, 2021].

### 3. Data and Methods

This research will integrate three methods, namely Fault Fracture Density (FFD), Ground Magnetic Method, and Gravity Satellite Method, to analyze the structure alleged to be the formation of Kepuhlegundi hot spring. The FFD method analyzes the density of a lineament based on the topographic shape of the research area. The topographic data utilizes DEMNAS (National Digital Elevation Model) data with an 8-meter resolution. This is a combination of several data sources, including IFSAR (5m resolution), TERRASAR-X (5m resampling resolution from the original resolution of 5–10 m), and ALOS PALSAR (11.25 m resolution) [Badan Informasi Geospasial, 2018]. The process of creating a lineament drawing involves converting elevation data from a DEM into a multidirectional hillshade. This allows for a clear visualization of the line's shape from eight different directions (0°, 45°, 90°, 135°, 180°, 235°, 270°, 315°). The calculation process of lineament density is based on the number and length of lineament in each grid area then the value on each grid will be contoured with the results in the form of a FFD map [Nahli *et al.*, 2016]. In this method, a cell size of 1×1 km is chosen because this size is quite effective in calculating the correlation between fracture density and geothermal features, in this case is hot springs [Soengkono, 1999]. The effect of selecting this cell size will have an impact on the level of exaggeration and smoothness of the density distribution calculated [Haeruddin *et al.*, 2016]. In this study, we used a grid size of 0.25×0.25 km and a pixel size of 0.25×0.25 to get a smoother distribution of values. The azimuth magnitude of each lineament was plotted on a rose diagram to identify trends in azimuth orientation in the Kepuhlegundi Hot Spring area [Nabhan *et al.*, 2024].

The Geotron Model G5 Proton Memory Magnetometer was used to measure ground magnetic data. Hills and community plantations dominate the measurement area, with hot springs located in the middle of the 90-hectare plot. The lot shape is determined by the orientation of the dominant structures in the study area. The measurement method employs the Base-Rover system with 50 to 70 meters between measurement points, resulting in 110 stations. During the measurement process, we perform data quality control by taking 5 to 7 iterations of data at the same location. Processing the magnetic data involves applying diurnal correction and IGRF (International Geomagnetic Reference Field) correction to obtain the Total Magnetic Intensity (TMI) value. The Reduce to Equator (RTE) filter process is used to transform the dipole anomaly into a monopole, ensuring that the anomaly is in its true position. [Baranov, 1957]. To separate residual and regional anomalies, a spectrum analysis stage is performed to determine the depth of each anomaly using an upward continuation filter.

The gravity method uses secondary data obtained via satellite, specifically GGM (Global Gravity Model) Plus. This model is the outcome of collaborative research between

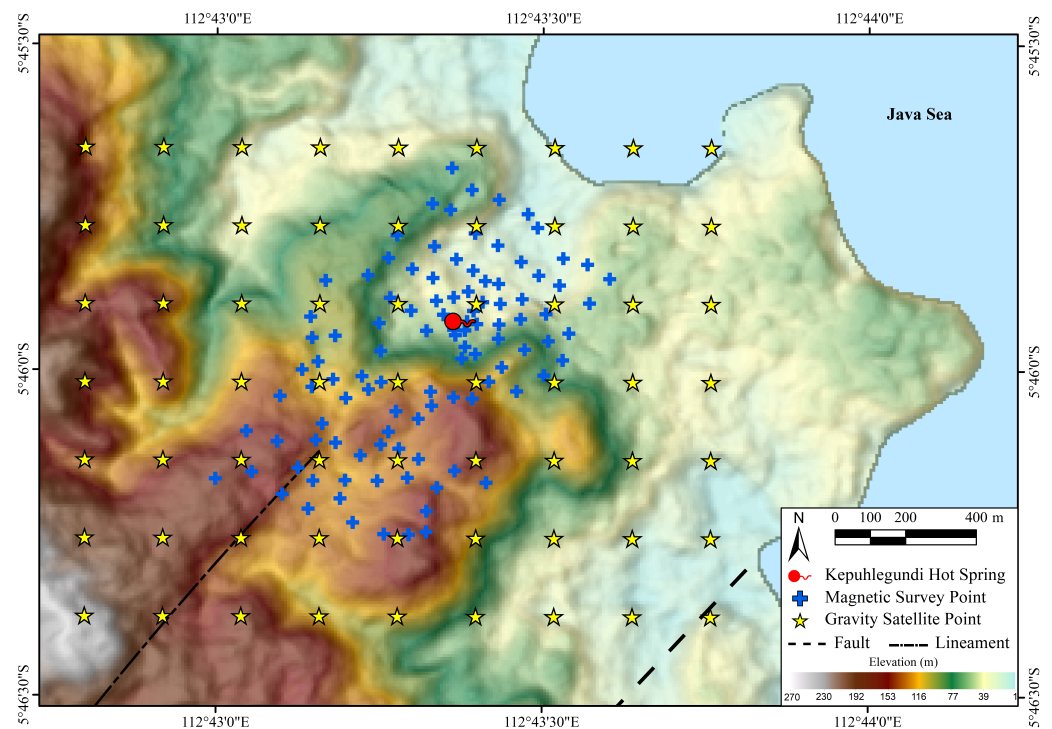


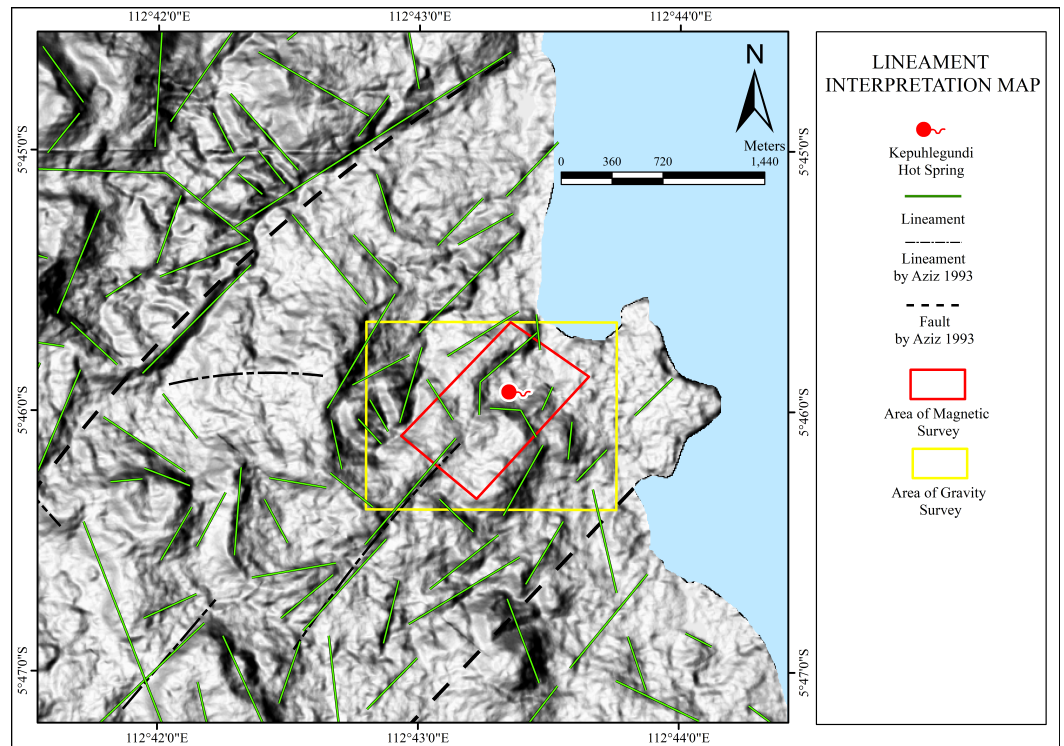
**Figure 3.** Topographic map of Kepuhlegundi Hot Spring along the positions of magnetic survey points (blue colored plus) and gravity satellite points (yellow-colored stars).

Curtin University and the Technical University of Munich. GGMplus is a composite of GRACE and GOCE satellite gravity, EGM2008 and short-wavelength topographic gravity effects at about 200 m resolution for all terrestrial and near-coastal areas of the Earth between  $\pm 60^\circ$  latitude [Hirt, Ch. et al., 2013]. 63 gravity data points are distributed across all lots in the magnetic method. The data obtained from GGMplus is in the form of gravity disturbance data, which is equivalent to a free air anomaly. Therefore, it is necessary to make corrections using the SRTM2gravity field correction model to obtain the Complete Bouguer Anomaly (CBA) [Pohan et al., 2023]. Data processing in the CBA separates residual and regional anomalies using the upward continuation method, which undergoes the same spectrum analysis stage as the magnetic method.

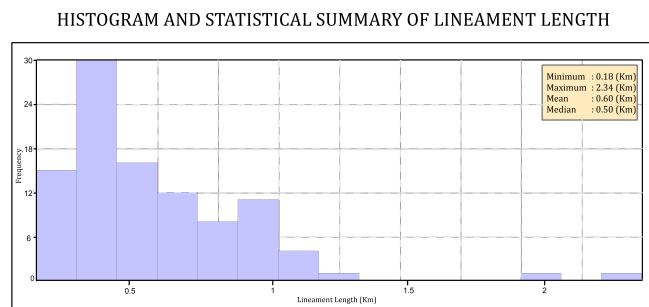
## 4. Results and Discussion

### 4.1. FFD Analysis

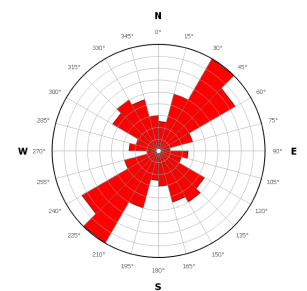
Fault Fracture Density (FFD) analysis is a way to look at the area and figure out where the weak spots are. It does this by counting how many dense lineaments there are in the area, which is caused by the geological structures in that area [Nayoan et al., 2023]. Based on the lineament interpretation (Figure 4a), the distribution of lineament structures around the hot springs and around the geological structures that have been previously identified. A total of 99 lineaments were interpreted with a length range of 0.18–2.34 km, and the average length was 0.60 km (Figure 4b). Based on the rose diagram (Figure 4c), the orientation of the interpreted lineaments tends to be parallel to the identified geological structures, dominated by the 30–45 NE direction. Lineaments with directions that tend to be the same as the regional geological structure can confirm that the research area is controlled by sinistral faults. The tendency of the same direction or parallel to the main structure is generally characterized by the strike-slip fault process that occurs in the area [Blenkinsop, 2008]. Therefore, it can be validated that the research area is controlled by sinistral fault and is in accordance with the mapped Meratus pattern structure.



(a)



(b)



(c)

**Figure 4.** a) Lineament interpretation map of the study area with 8 directions of shading/multidirectional hillshade; b) Histogram and statistical summary of lineament length; c) Lineament orientation in study area by rose diagram.

The result of FFD analysis shows the distribution of the density value of the lineament, which has been interpreted in the form of a map (Figure 5), with the range of value in the research area known as 0–4.45 km/km<sup>2</sup>. The area around the hot springs is in an area with a high FFD value, which is around 2.88–3.93 km/km<sup>2</sup>. The increase in value is consistent with the geological structures discovered near the springs. This is because the destruction process weakens the area around the geological structure, creating a weak zone, whereas coastal areas and alluvial plains have undergone a sedimentation process that can cover traces of the destruction process [Manyo and Hutagalung, 2022]. High densities are dominant in the vicinity of geological structures such as faults, while small densities tend to occur in coastal areas or alluvial plains. With high FFD, the zone can become highly permeable, making it easier for fluids to flow through the cracks [Arrofi et al., 2022].

**4.2. Magnetic Method**

The total magnetic intensity (TMI) map is generated by applying the Krigging interpolation method to each magnetic measurement point in the field. The Reduce to Equator

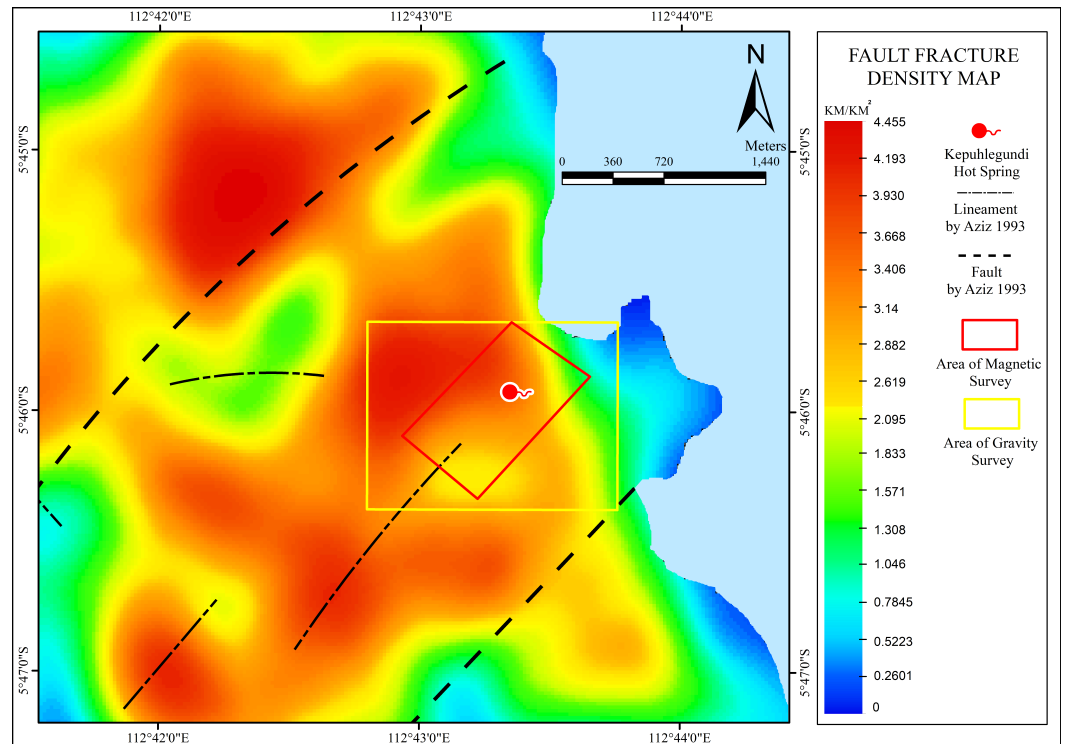


**Figure 5.** Fault Fracture Density (FFD) map of the Kepuhlegundi hot spring area with geological structures based on the Bawean geological map.

(RTE) process is then used to get rid of the dipole effect in the study area. This makes sure that the anomaly is in the right place (Figure 6). Anomalies on the TMI map reflect changes on the RTE map, indicating the withdrawal of anomalies that tend to shift in the north-south direction. This may be because of the magnetic field inclination in the research area [Araffa et al., 2018]. The magnetic anomaly distribution expresses the level of susceptibility or the ability to be magnetized in units of nT (nano Tesla).

According to the RTE map, the magnetic anomaly values in the study area range from  $-1044$  to  $126$  nT. The distribution of anomalous values in the research area is quite varied. This may indicate that the area is geologically complex and influenced by geological structures. Compared to literature on geothermal studies of hot springs, the magnetic anomaly in this study area typically exhibits lower magnitudes. This may be due to the fact that the research area is situated in a region with rock formations resulting from volcanic eruptions, with bedrock taking the form of limestone.

The Radial Average Spectrum technique can determine the condition of regional and residual anomalies at different depths. The Fast Fourier Transform (FFT) process calculates this technique [Basantaray and Mandal, 2022]. Applying the Fast Fourier Transform (FFT) converts magnetic field data from the spatial domain to the frequency domain. This allows for the separation of regional and residual anomalies based on the breakdown of slope data. Figure 7 shows the spectrum analysis results in the form of a regional linear line (orange line) with an anomaly depth of 78 meters and a residual linear line (blue line) with an anomaly depth of 14 meters.

The magnetic anomaly in the research area was determined using the upward continuation filter process. This process involves lifting the data to a certain height to eliminate interference effects. According lifting height is twice the depth of the anomaly, as determined from the spectrum analysis [Arellano et al., 2021]. Figure 8a shows the research area's regional anomaly following the upward continuation process up to 156 meters. The anomaly exhibits a regional and uncomplicated distribution, with values ranging from  $-470$  to  $-341$  nT. The hot springs are situated in an area with a medium anomaly between the high and low regional anomalies. However, there are no significant regional

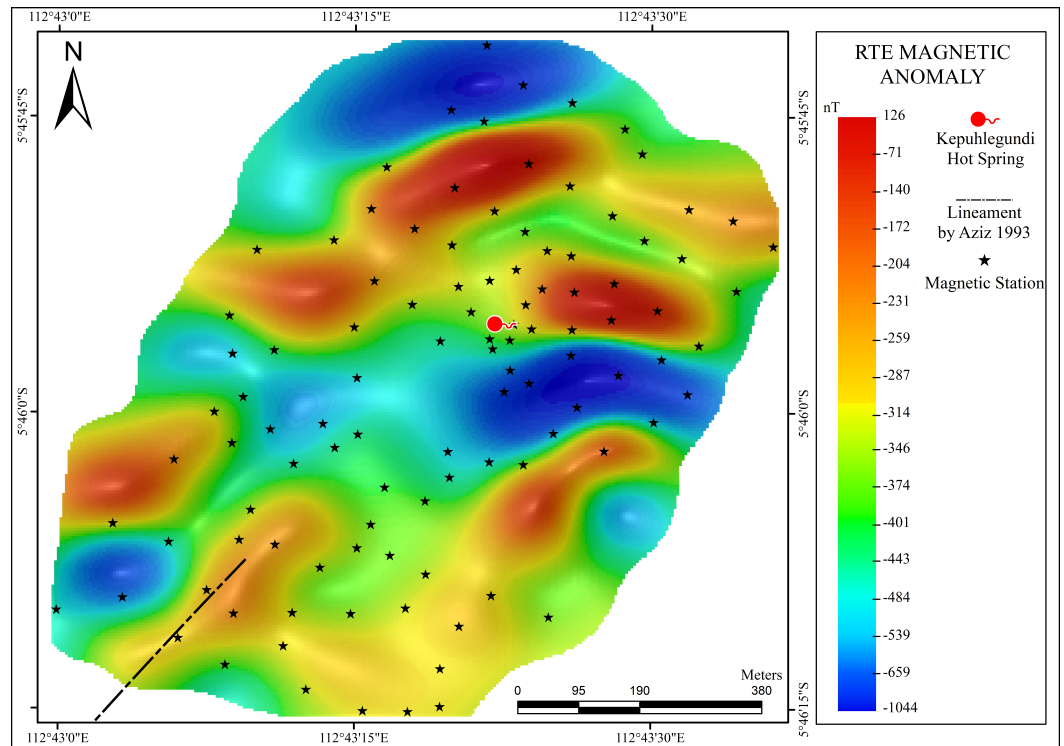


**Figure 6.** Magnetic anomaly map after Reduce to Equator (RTE) filter in the Kepuhlegundi Hot Spring area with lineament by Bawean geological map.

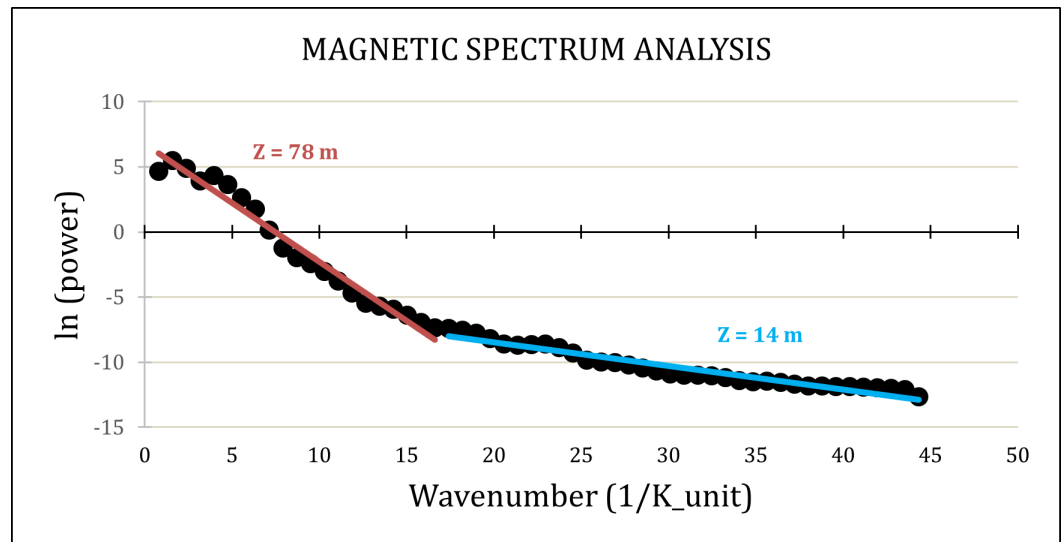
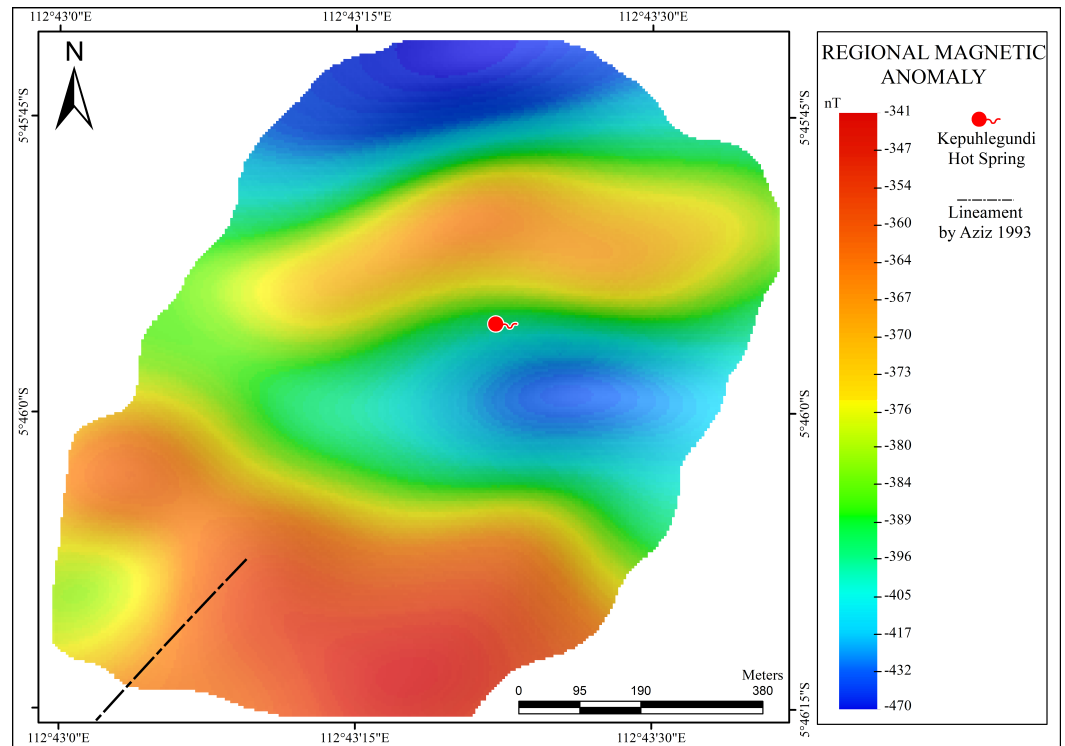


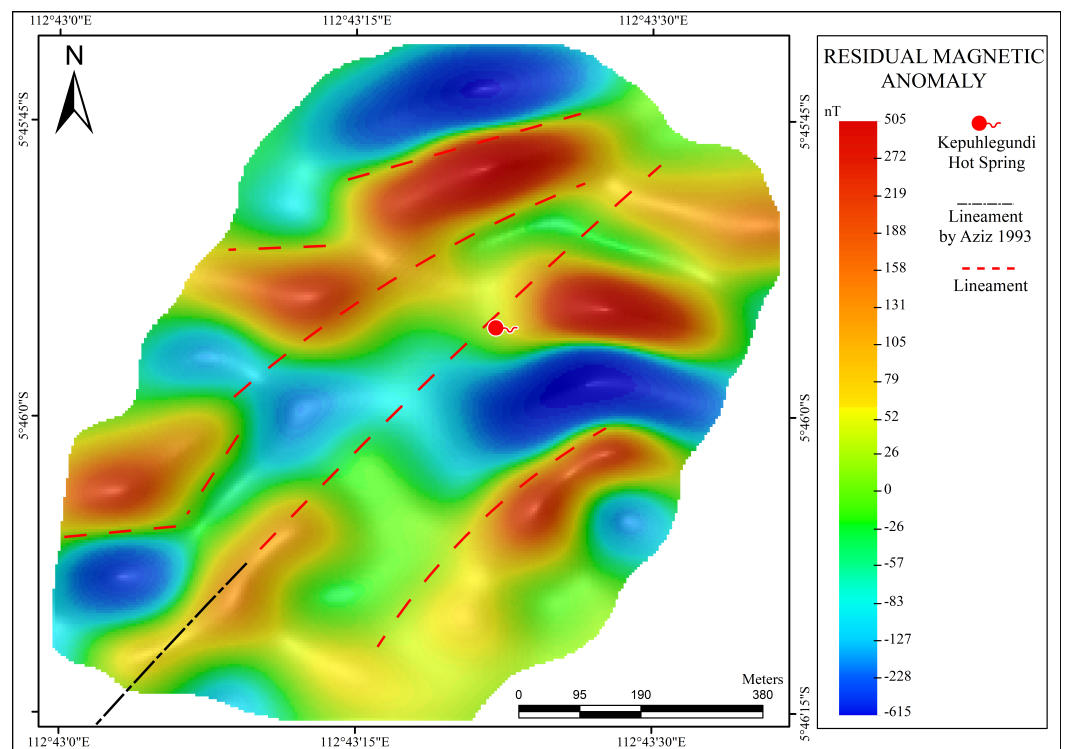
**Figure 7.** Spectral Analysis from magnetic processing for separation and depth identify of regional and residual anomaly.

anomalies on the structural lineament of the geological map. This suggests that the structures and hot springs did not form at a significant depth. At a depth of 78 meters, the low magnetic anomaly value indicates that the area being researched is already part of the bedrock of Bawean Island, specifically the gelam limestone. This suggests a strong correlation between the research area and the island's bedrock. Magnetic residual anomalies are geological anomalies at shallow depths that result from the removal of regional effects on the RTE map or the difference between the RTE map and the regional anomaly (Residual Anomaly = RTE Anomaly – Regional Anomaly) [Chouhan et al., 2022].





(a)



(b)

**Figure 8.** a) Regional anomaly magnetic map; b) Residual anomaly magnetic map of the Kepuhlegundi hot spring area with geological structures and lineament indicated by magnetic measurements (red dashed line) and lineament from Bawean geological map (black dashed line).

Figure 8b shows a distribution of residual anomalies that is highly variable with anomalous values ranging from  $-615$  to  $505$  nT. High magnetic anomalies indicate that the subsurface rock response in the research area has a high content of magnetic minerals

such as Fe. Igneous rocks with a high Fe composition, such as lava, basaltic, or andesitic, typically exhibit a high magnetic response. Upon examining the previously mapped geology distribution, we find that the research area falls within the volcanic rock region. Therefore, we can interpret the high anomaly (from 200 to 505 nT in the hot water area as indicating volcanic rocks, such as lava. Then, in areas with low anomalies (from  $-80$  to  $-615$  nT), it can be indicated by sedimentary rocks, with the case in this study being limestone or deposits formed from the hot springs themselves, namely travertine deposits with a magnetic mineral composition that tends to be low. In addition, anomalies that tend to be moderate (from  $-26$  to 100 nT) can be interpreted as the result of volcanic rocks in the form of tuff deposits. At the hot spring point, a demagnetization phenomenon occurs which makes the magnetic anomaly tend to be low in the vicinity due to the hot temperature. The geologic structure is interpreted by the boundary between the low and high magnetic anomalies, marked by the dashed red line in Figure 7b. The geologic map's lineament (black dashed line) outlines the region of anomalous contrast that exhibits a northeast-southwest trend. A significant change in anomaly value, assuming a sudden difference in rock type that characterizes the existence of a geological structure, leads to the interpretation of the boundary as a structure. The structure's is also indicated by the presence of anomalies that have the same value and are separated by what is believed to be the structure's alignment. The hot spring is indicated to have formed due to the structure continuity passing through the hot spring point.

#### 4.3. Gravity Method

The satellite gravity method makes a map of where the Complete Bouguer Anomaly (CBA) is found. The map is measured in milligals (mGal), which are related to how dense a rock is [Hinze et al., 2013]. Figure 8 illustrates that the anomalies' distribution varies within a range of  $-470$  to  $-341$  mGal. This similarity with the magnetic anomalies' results is due to the complex geological conditions and structures in the research area. When observing the values (Figure 9), it can be noted that hot springs are typically found in areas with moderate anomalies, even between areas with low or high anomaly contrasts. Based on the geological map, the lineament is a moderate anomaly. The rock's density affects the gravity anomaly's value. A high anomaly indicates a higher density closer to the surface, whereas a smaller anomaly indicates a lower density farther from the surface [Amir et al., 2021].

The distribution map of CBA is still affected by regional anomalies in the research area. Therefore, it should be separated into regional and residual anomalies, like the magnetic method, using the Radial Average Spectrum. The spectrum analysis results (Figure 10) indicate that the regional gravity anomaly in the research area is located at a depth of 139 meters, while the residual anomaly is at a depth of 86 meters.

The regional gravity anomaly is obtained by upward continuation, similar to the magnetic method. Spectrum analysis determines the depth. The regional gravity anomaly (Figure 11a) shows a regional and similar distribution of anomalies, with anomalies ranging from 26.47 to 30.23 mGal. Anomalies with high values are interpreted as bedrock in the research area, specifically gelam limestone with high density. The lack of anomalous hot springs and geological structures in the study area suggests that such features did not form at this depth.

The residual anomaly is determined using the same method as for the magnetic anomaly by separating the CBA from the regional anomaly. The results of the residual anomaly (Figure 11b) show a varied distribution of anomalies, with anomalous values ranging from  $-2.78$  to 3.11 mGal. Removing the influence of regional anomalies has resulted in a shallow anomaly, making the anomaly value relatively small compared to the CBA. The variation of the gravity anomaly will follow the distribution of rock types in the research area by looking at the different density values of each rock. In this study area, high anomalous values (from 0.79 to 3.11 mGal) are interpreted as rocks with a high density, as in the geologic conditions which tend to be volcanic rocks with the possibility of lava or breccia igneous rocks. Near the hot springs, previously magnetic was interpreted as sedimentary rock in the form of travertine deposits from the hot springs themselves, this is

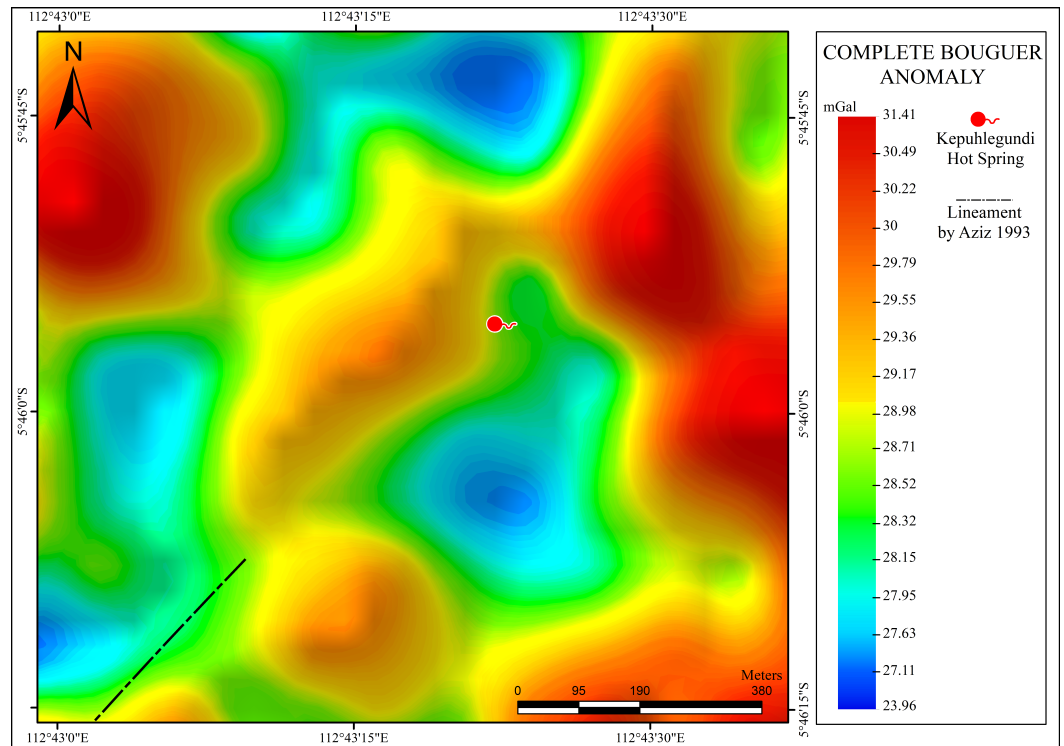


**Figure 9.** Complete Bouguer Anomaly (CBA) map of the Kepuhlegundi hot spring with lineament by Bawean geological map.

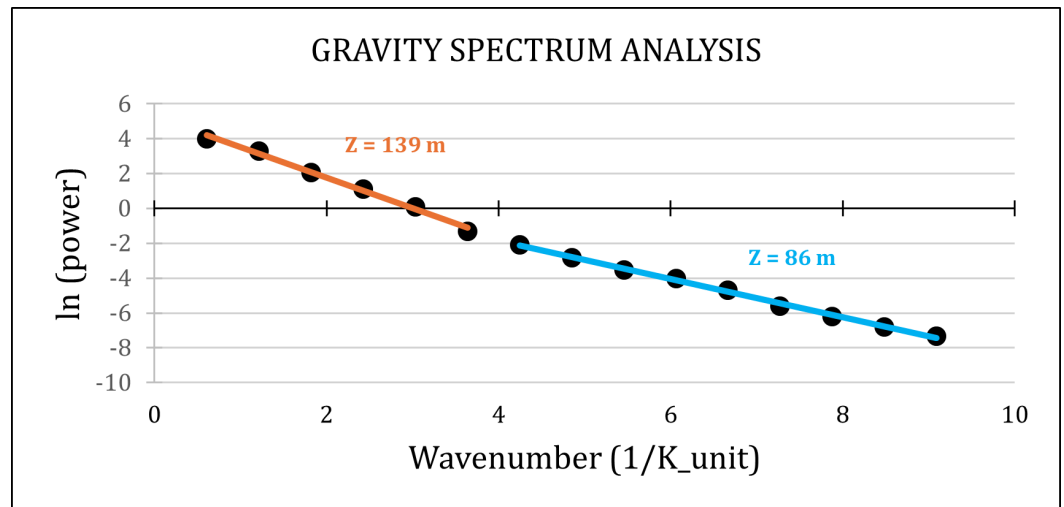
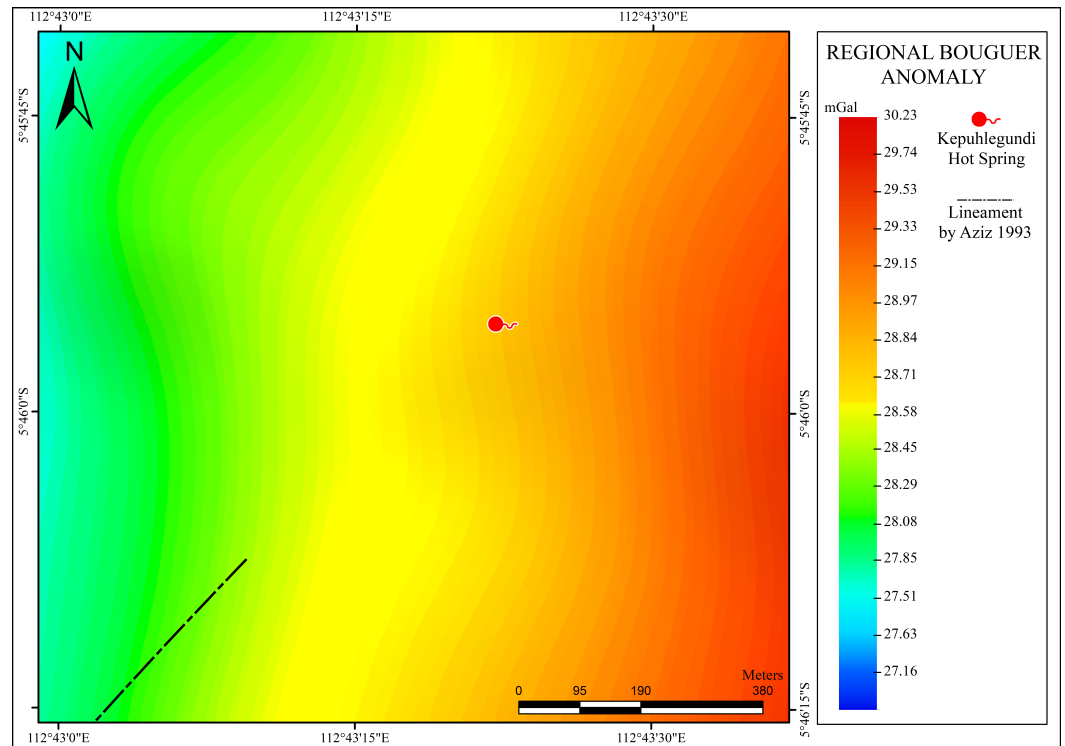


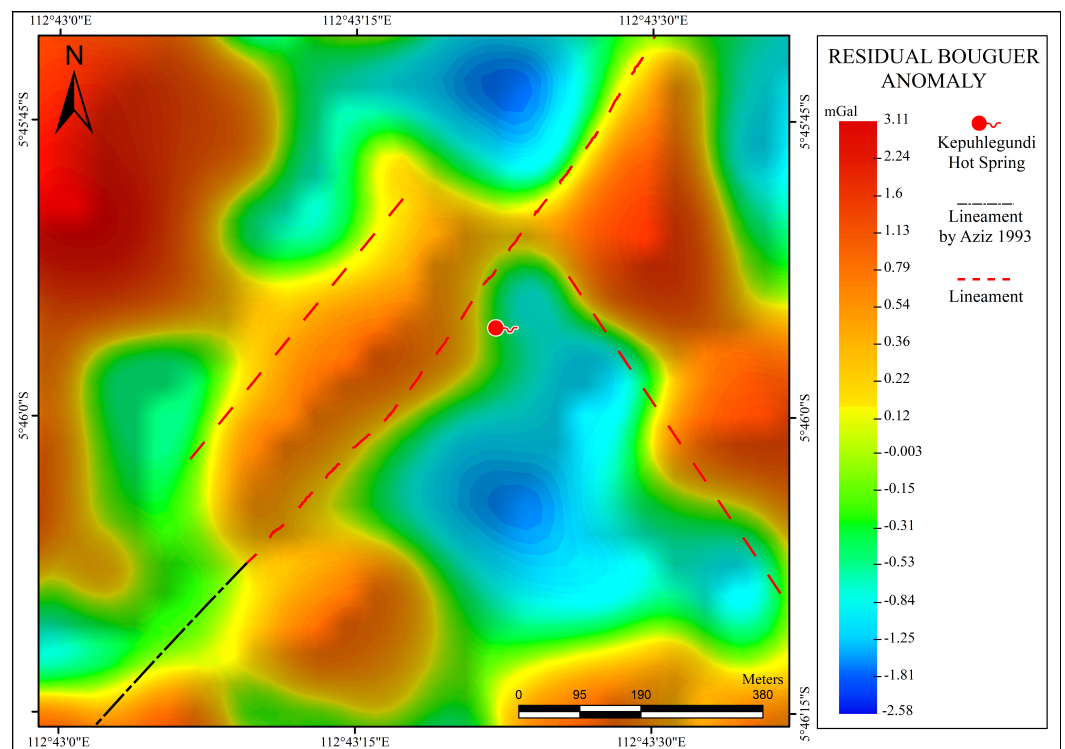
**Figure 10.** Spectral Analysis from gravity processing for separation and depth identify of regional and residual anomaly.

evidenced by the low anomaly results (from 0 to  $-2.81$  mGal), which are rocks with low density levels. The residual anomaly contrasts with the anomaly at the hot spring but has the same continuity as the geological structure in the study area, which runs northeast-southwest. The geologic map lineament (black line) is thought to be continuous because the contrast between low and high anomalies is long. This suggests that rock lithology is different between the anomalous values. The presence of contrasting lithological variations along a straight line with a consistent trend may suggest a geological structure in the area. Geological structures control the formation of hot springs.

The study employed three effective methods for identifying regional geological structures. The FFD method is particularly useful for mapping weak zones influenced by structural control, while the magnetic and gravity methods are effective at identifying



(a)



(b)

**Figure 11.** a) Regional anomaly map; b) Residual anomaly map from gravity satellite in the Kepuhlegundi hot spring area with geological structures and lineament indicated by magnetic measurements (red dashed line) and lineament from Bawean geological map (black dashed line).

anomalous contrast boundaries that indicate geological structures in each area. The structures found in the three methods show a dominant direction of northeast-southwest, with a focus on the study area. The structure's orientation matches that of Bawean Island's

geological structure, as described by [Aziz *et al.*, 1993] on the Regional Geological Map of Bawean Sheet. The Meratus pattern may influence Bawean Island's geological structure and show indications of a sinistral fault, as suggested by [Arifin and Lugra, 2016].

The study integrated magnetic and gravity methods to determine the location of the structure in the hot spring area. It was found that the structure is in a residual anomaly or at a shallow depth, indicating that it was formed after the end of the Miocene period, during which the bedrock of Bawean Island, specifically the gelam limestone formation, was formed. The formation of Kepuhlegundi Hot Spring is controlled by geological structures in the form of continuous fractures (Figure 12) based on the analysis of the continuity and weak zones around the hot spring by each method. The effect of fractures on the formation of hot springs is due to the surrounding weak zone increasing the permeability of the rock so that hot fluids will be very easily to pass through [Rafi *et al.*, 2023; Zhou *et al.*, 2023]. In addition, the structure passes through areas with high magnetic and gravity anomalies that may indicate the presence of solid volcanic rock. This could potentially facilitate heating of the aquifer through the fracture zone. By integrating spatial and geophysical analyses, it is possible to validate the relationship between the identified regional geological structures and the formation of Kepuhlegundi Hot Spring. Furthermore, this study can serve as an initial illustration for further investigation of Kepuhlegundi Hot Spring's subsurface conditions.

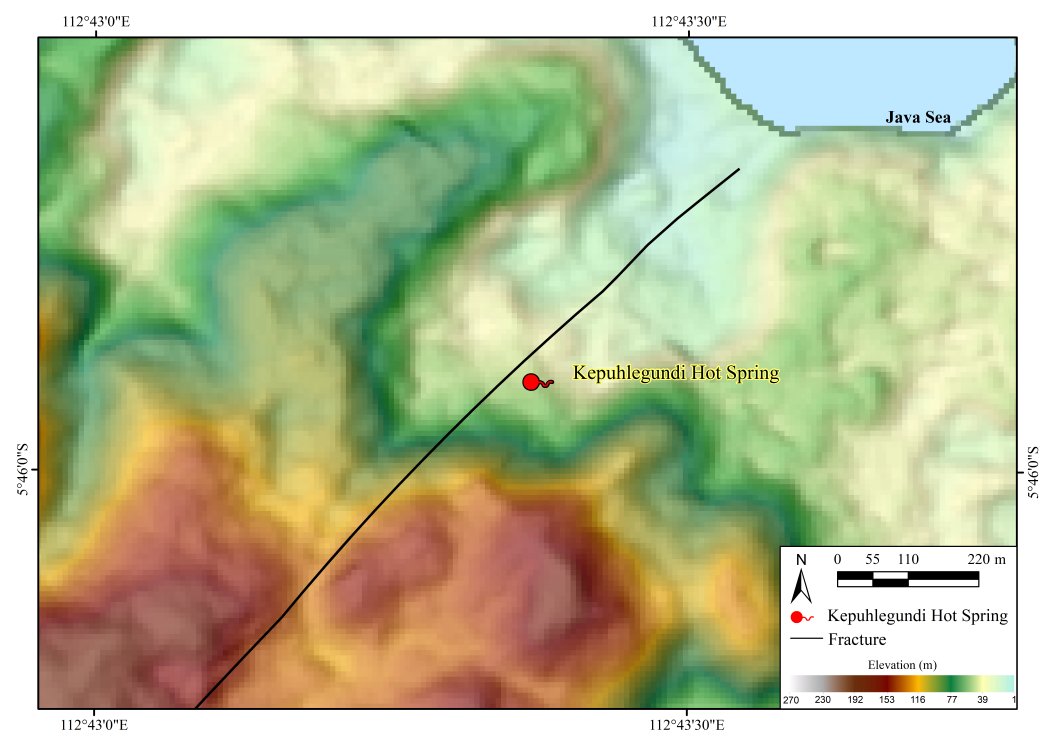


**Figure 12.** Map of the results of identifying the structural continuity that controls the formation of Kepuhlegundi hot springs from the integration of magnetic, gravity satellite, and fault fracture density (FFD) methods.

## 5. Conclusion

The Kepuhlegundi Hot Spring formation can be identified by analyzing and integrating three methods: FFD, magnetic, and gravity. The surface geological structure controls this formation. The FFD analysis method can accurately identify weak zones around the hot springs by analyzing the geological structures in the study area. This is achieved by mapping the dense lineaments caused by these structures. Magnetic and gravity methods can be used to determine the location and orientation of structures based on the contrast of low and high anomalies that extend through the hot springs. Both methods predict that

the controlling structure is at a shallow depth, between 15 to 80 meters below the surface. This prediction is based on an analysis of both residual and regional anomalies. The orientation of the structure formed at Kepuhlegundi Hot Spring is consistent with the Meratus Structure Pattern, which runs in a northeast-southwest direction. This suggests that the structure was formed by the Meratus pattern, as confirmed by the potential method and FFD analysis. This research can be the first step in further investigation into the subsurface conditions around hot springs, particularly the geological structure.

**Acknowledgments.** The authors gratefully acknowledge financial support from the Institut Teknologi Sepuluh Nopember for this work, under project scheme of the Publication Writing and IPR Incentive Program (PPHKI) 2024.

## References

- Alvarez, R., and V. Yutsis (2015), Southward Migration of Magmatic Activity in the Colima Volcanic Complex, Mexico: An Ongoing Process, *International Journal of Geosciences*, 06(09), 1077–1099, <https://doi.org/10.4236/ijg.2015.69085>.
- Amir, H., S. Bijaksana, D. Dahrin, et al. (2021), Subsurface structure of Sumani segment in the Great Sumatran Fault inferred from magnetic and gravity modeling, *Tectonophysics*, 821, 229,149, <https://doi.org/10.1016/j.tecto.2021.229149>.
- Araffa, S. A. S., M. El-bohoty, M. Abou Heleika, et al. (2018), Implementation of magnetic and gravity methods to delineate the subsurface structural features of the basement complex in central Sinai area, Egypt, *NRIAG Journal of Astronomy and Geophysics*, 7(1), 162–174, <https://doi.org/10.1016/j.nrjag.2017.12.002>.
- Arellano, C. J. J., L. T. Armada, C. B. Dimalanta, K. L. Queaño, E. S. Andal, and G. P. Yumul (2021), Interpretation of ground magnetic data in Suyoc, Mankayan Mineral District, Philippines, *Resource Geology*, 71(4), 363–376, <https://doi.org/10.1111/rge.12270>.
- Arifin, L., and W. Luga (2016), Zona Sesar di Perairan Kalimantan Selatan, *Jurnal Geologi Kelautan*, 7(1), <https://doi.org/10.32693/jgk.7.1.2009.166>.
- Arrofi, D., I. S. Abu-Mahfouz, and S. D. Prayudi (2022), Investigating high permeable zones in non-volcanic geothermal systems using lineament analysis and fault fracture density (FFD): northern Konawe Regency, Indonesia, *Geothermal Energy*, 10(1), <https://doi.org/10.1186/s40517-022-00241-3>.
- Aziz, S., S. Hardjoprawiro, and A. Mangga (1993), Geological Map of the Bawean Island and Masalembo Quadrangle, Jawa.
- Badan Informasi Geospasial (2018), Seamless digital elevation model (DEM) dan Batimetri Nasional, <https://tanahair.indonesia.go.id/demnas/>, (visited on 2024).
- Baranov, V. (1957), A New Method for Interpretation of Aeromagnetic Maps: Pseudo-Gravimetric Anomalies, *Geophysics*, 22(2), 359–382, <https://doi.org/10.1190/1.1438369>.
- Basantaray, A. K., and A. Mandal (2022), Interpretation of gravity-magnetic anomalies to delineate subsurface configuration beneath east geothermal province along the Mahanadi rift basin: a case study of non-volcanic hot springs, *Geothermal Energy*, 10(1), <https://doi.org/10.1186/s40517-022-00216-4>.
- Bense, V. F., T. Gleeson, S. E. Loveless, O. Bour, and J. Scibek (2013), Fault zone hydrogeology, *Earth-Science Reviews*, 127, 171–192, <https://doi.org/10.1016/j.earscirev.2013.09.008>.
- Blenkinsop, T. G. (2008), Relationships between faults, extension fractures and veins, and stress, *Journal of Structural Geology*, 30(5), 622–632, <https://doi.org/10.1016/j.jsg.2008.01.008>.
- Choi, J.-H., P. Edwards, K. Ko, and Y.-S. Kim (2016), Definition and classification of fault damage zones: A review and a new methodological approach, *Earth-Science Reviews*, 152, 70–87, <https://doi.org/10.1016/j.earscirev.2015.11.006>.
- Chouhan, A. K., S. Chopra, H. Chaube, D. Singh, and A. K. Mishra (2022), Integrated analysis of the gravity and the magnetic data to infer structural features and their role in prospective mineralisation in and around the Ambaji-Deridanta-Chitrasani region, NW India, *Journal of Earth System Science*, 131(4), <https://doi.org/10.1007/s12040-022-01979-x>.

- Danakusumah, G., and Suryantini (2020), Integration of the Lineament Study in the Karaha-Bodas Geothermal Field, West Java, *IOP Conference Series: Earth and Environmental Science*, 417(1), 012,008, <https://doi.org/10.1088/1755-1315/417/1/012008>.
- Fajar, M. H. M., D. D. Warnana, A. Widodo, S. E. Prabawa, and A. Iswahyudi (2021), Aquifer System Analysis to Identify the Cause of Groundwater Depletion at Umbulan Spring, Indonesia, *Chemical Engineering Transactions*, 89, 385–390, <https://doi.org/10.3303/CET2189065>.
- Haeruddin, A. Saepuloh, M. N. Heriawan, and T. Kubo (2016), Identification of linear features at geothermal field based on Segment Tracing Algorithm (STA) of the ALOS PALSAR data, *IOP Conference Series: Earth and Environmental Science*, 42, 012,003, <https://doi.org/10.1088/1755-1315/42/1/012003>.
- Hafizh, M. (2022), Vulkanostratigrafi Dan Petrogenesis Pulau Bawean: Studi Khusus Pada Daerah Danau Kastoba Dan Sekitarnya, Pulau Bawean, Kabupaten Gresik, Jawa Timur, *Perpustakaan Digital - Digilib ITB*.
- Hamilton, W. (1974), *Earthquake Map Of The Indonesian Region*, US Geological Survey, <https://doi.org/10.3133/i875c>.
- Hendratno, A., and F. D. Khoir (2019), Petrologi Batuan Vulkanik Pulau Bawean, Kabupaten Gresik, Jawa Timur, in *Seminar Nasional Kebumihan KE-12 Teknik Geologi, Fakultas Teknik, Universitas Gadjah Mada*.
- Hinze, W. J., R. Ralph, R. von Frese, H. Afif, and A. H. Saad (2013), *Gravity and Magnetic Exploration: Principles, Practices, and Applications*, Cambridge University Press.
- Hirt, Ch., S. Claessens, T. Fecher, M. Kuhn, R. Pail, and M. Rexer (2013), New ultrahigh-resolution picture of Earth's gravity field, *Geophysical Research Letters*, 40(16), 4279–4283, <https://doi.org/10.1002/grl.50838>.
- Hosono, T., and C. Yamanaka (2021), Origins and pathways of deeply derived carbon and fluids observed in hot spring waters from non-active volcanic fields, western Kumamoto, Japan, *Earth, Planets and Space*, 73(1), <https://doi.org/10.1186/s40623-021-01478-1>.
- Hutubessy, S. (2003), Struktur Sesar Bawah Permukaan dan Implikasinya Terhadap Pemunculan Kelompok Gunungapi di Semenanjung Muria, Jawa Tengah, Berdasarkan Pendekatan Analisis Gaya Berat, *Jurnal Geologi dan Sumberdaya Mineral*, 9(133), 37–54.
- Keegan-Treloar, R., D. J. Irvine, S. C. Solórzano-Rivas, A. D. Werner, E. W. Banks, and M. J. Currell (2022), Fault-controlled springs: A review, *Earth-Science Reviews*, 230, 104,058, <https://doi.org/10.1016/j.earscirev.2022.104058>.
- Luo, L., H. Wen, and E. Capezzuoli (2021), Travertine deposition and diagenesis in Ca-deficiency perched hot spring systems: A case from Shihuadong, Tengchong, China, *Sedimentary Geology*, 414, 105,827, <https://doi.org/10.1016/j.sedgeo.2020.105827>.
- Manyoe, I. N., and R. Hutagalung (2022), The extraction and analysis of lineament density from digital elevation model (dem) in libungo geothermal area, gorontalo, *IOP Conference Series: Earth and Environmental Science*, 1089(1), 012,012, <https://doi.org/10.1088/1755-1315/1089/1/012012>.
- Nabhan, M. H., M. H. M. Fajar, and W. Lestari (2024), Analysis of Geological Structure based on 3D Virtual Outcrop Model and Physical Properties of Rocks in Wringinanom District, Gresik Regency, *IOP Conference Series: Earth and Environmental Science*, 1307(1), 012,024, <https://doi.org/10.1088/1755-1315/1307/1/012024>.
- Nahli, K., F. Mulyana, G. E. Tsani, M. A. Alwan, M. H. Darajat, and R. N. Hendrawan (2016), Identifying Non-Volcanic Geothermal Potential in Amohola, Southeast Sulawesi Province, by Applying the Fault and Fracture Density (FFD) Method, *IOP Conference Series: Earth and Environmental Science*, 42, 012,015, <https://doi.org/10.1088/1755-1315/42/1/012015>.
- Nayoan, A. G. P., K. A. Pranatikta, Anil, F. Hendrasto, and S. Yuniasih (2023), Upflow-outflow Zone Identification Based on Geochemistry Indicator and Fault Fracture Density Correlation Analysis in Mt. Gede Geothermal Case, West Java, *IOP Conference Series: Earth and Environmental Science*, 1159(1), 012,003, <https://doi.org/10.1088/1755-1315/1159/1/012003>.

- Pohan, A. F., S. Sismanto, B. E. Nurcahya, et al. (2023), Utilization and modeling of satellite gravity data for geohazard assessment in the Yogyakarta area of Java Island, Indonesia, *Kuwait Journal of Science*, 50(4), 499–511, <https://doi.org/10.1016/j.kjs.2023.05.016>.
- Pulonggono, A. D., and S. Martodjojo (1994), Perubahan tektonik Paleogen-Neogen merupakan peristiwa tektonik terpenting di Jawa, in *Geologi dan Geotek Pulau Jawa, Yogyakarta*, pp. 37–39.
- Puswanto, E., A. Farisan, D. A. Wibowo, et al. (2022), Fault Bend Fold Related Thrust Fault Waturanda Formation as Representative of Tectonic Compression as an Asset Geological Heritage of GNKK, Indonesia, in *2022 IEEE Asia-Pacific Conference on Geoscience, Electronics and Remote Sensing Technology (AGERS)*, IEEE, <https://doi.org/10.1109/AGERS56232.2022.10093295>.
- Rafi, M. E. D., M. H. M. Fajar, M. S. Purwanto, et al. (2023), Analysis of Formation Ronggojalu Spring and Probolinggo Active Fault Continuity with Satellite Data Gravity Method, *Jurnal Penelitian Pendidikan IPA*, 9(10), 8456–8461, <https://doi.org/10.29303/jppipa.v9i10.3399>.
- Rosli, N. A., M. N. A. Anuar, M. H. Mansor, N. S. I. Abdul Rahim, and M. H. Arifin (2022), What Makes A Hot Spring, Hot?, *Warta Geologi*, 48(1), 30–35, <https://doi.org/10.7186/wg481202204>.
- Setijadji, L. D., S. Kajino, A. Imai, and K. Watanabe (2006), Cenozoic Island Arc Magmatism in Java Island (Sunda Arc, Indonesia): Clues on Relationships between Geodynamics of Volcanic Centers and Ore Mineralization, *Resource Geology*, 56(3), 267–292, <https://doi.org/10.1111/j.1751-3928.2006.tb00284.x>.
- Shiraishi, F., A. Morikawa, K. Kuroshima, et al. (2020), Genesis and diagenesis of travertine, Futamata hot spring, Japan, *Sedimentary Geology*, 405, 105,706, <https://doi.org/10.1016/j.sedgeo.2020.105706>.
- Sidarto, N. S., and P. Sanyoto (1999), Sistem sesar Pengontrol Pemunculan Kelompok Gunungapi Muria Hasil Penafsiran Citra Landsat, *Jurnal Geologi dan Sumberdaya Mineral*, IX(99).
- Siringoringo, L. P., B. Sapiie, A. Rudyawan, and I. G. B. E. Sucipta (2024), Origin of high heat flow in the back-arc basins of Sumatra: An opportunity for geothermal energy development, *Energy Geoscience*, 5(3), 100,289, <https://doi.org/10.1016/j.engeos.2024.100289>.
- Sismanto, S., U. Yasmita, and F. Jusmi (2018), Interpretation of the gravity and magnetic anomalies of the geothermal subsurface structure area in Pamancalan, Lebak, Banten, West Java, Indonesia, *Arabian Journal of Geosciences*, 11(14), <https://doi.org/10.1007/s12517-018-3740-y>.
- Soengkono, S. (1999), Te Kopia geothermal system (New Zealand) - the relationship between its structure and extent, *Geothermics*, 28(6), 767–784, [https://doi.org/10.1016/S0375-6505\(99\)00042-5](https://doi.org/10.1016/S0375-6505(99)00042-5).
- Suprijadi, B. (1992), Peranan Wrench Fault Pada Akumulasi Hidrokarbon di Pulau Madura, in *Proc. of the 21th Annual Scientific Meeting of the Indonesian Association of Geologist*.
- Usman, E. (2012), Tektonik Dan Jalur Vulkanik Busur Belakang Baweanmuria Sebagai Pengontrol Pembentukan Cekungan Pati Dan Potensi Hidrokarbon, *Indonesian Journal of Applied Sciences*, 2(3).
- Usman, E., A. Sudradjat, E. R. Suparka, and I. Syafri (2010), Pembentukan Jalur Vulkanik Busur Belakang Muria-Bawean Dan Pengaruhnya Terhadap Pembentukan Cekungan Pati, in *PRECEEDINGS PIT IAGI LOMBOK 2010. The 29th IAGI Annual Convention and Exhibition*.
- van Bemmelen, R. W. (1949), *The Geology of Indonesia. Vol. IA: General Geology of Indonesia and Adjacent Archipelagoes*, Government Printing Office, The Hague.
- Zhou, X., L. Zhuo, Y. Wu, G. Tao, J. Ma, et al. (2023), Origin of some hot springs as conceptual geothermal models, *Journal of Hydrology*, 624, 129,927, <https://doi.org/10.1016/j.jhydrol.2023.129927>.